X-ray spectral evolution of TeV HBLs with BeppoSAX, XMM-Newton and SWIFT

F. Massaro[1,3], A. Tramacere[2], A. Cavaliere[3], M. Perri[4], P. Giommi[4]

[1] *Harvard, Smithsonian Astrophysical Observatory, 60 Garden St., Cambridge, MA 02138*
[2] *Stanford Linear Accelerator Center, 2575 Sand Hill Road, Menlo Park, CA 94025*
[3] *Department of Physics, 'Tor Vergata University' of Roma, Roma, Italy*
[4] *ASI Science Data Center (ASDC), Roma, Italy*

Abstract

Many of the extragalactic sources detected at TeV energies are BL Lac objects; the majority belong to the subclass of "high frequency peaked BL Lacs" (HBLs) with spectral energy distributions (SEDs) exhibiting a first peak in the X-ray band. At a closer look, their X-ray spectra appear to be generally curved into a log-parabolic shape; investigating Mrk 421, two correlations were found between the spectral parameters. One involves the height S_p of the SED, that increases with the position E_p of the first peak, interpreted as a signature of synchrotron radiation; the other involves the curvature parameter b decreasing as E_p increases, interpreted in terms of statistical/stochastic acceleration processes for the emitting electrons. Here we report the X-ray analysis of all TeV HBLs observed till April 2007 to pinpoint their behaviours in the $E_p - S_p$ and $E_p - b$ planes and to compare them with Mrk 421.

1 Introduction

A recent analysis of Mrk 421 observations performed with *BeppoSAX*, *XMM-Newton* and ASCA (Tramacere et al. 2007, A&A, 466, 521) has shown two correlations between spectral parameters. These are relevant as signatures of synchrotron emission and of statistical/stochastic acceleration mechanisms for the emitting electrons, respectively. Here, we look for any similar correlations or trends in other TeV HBLs, reporting three examples among the selected sample: 1H 1426+428, Mrk 501 and PKS 2155-304.

2 Spectral analysis

We describe the X-ray continuum with a log-parabolic model (Landau et al. 1986, ApJ, 308, L78; Massaro et al. 2004, A&A, 422, 103).
The log-parabolic model is tested under the form

$$F(E) = K\ E^{-a-b\ log(E)} \quad [photons\ cm^{-2}\ s^{-1}\ keV^{-1}], \qquad (1)$$

or the alternative SED representation

$$S(E) = S_p\ 10^{-b\ log^2(E/E_p)} \qquad (2)$$

with $S_p = E_p^2\,F(E_p)$. After Eq. (2), the values of the parameters E_p (the location of the SED energy peak), S_p (the peak height), and b (the curvature parameter) can be estimated independently in the fitting procedure (Tramacere et al. 2007a). Details of the spectral analysis and comparison with other models are also presented in Massaro et al. (2008, A&A, 478, 395).

3 Results

In the case of Mrk 421 Tramacere et al. (2007, A&A, 466, 521) found that the SED peak energy E_p correlates with the peak flux S_p but anticorrelates with the curvature parameter b. To compare the observed quantities (E_p, b and S_p) among different sources, it is necessary to make cosmological corrections.
The curvature parameter b is not afffected while the other parameters, E_p and S_p, are. The rest frame energy peak E_p^* is given by: $E_p^* = (1+z)\ E_p$. As the value of S_p is proportional to the bolometric emitted flux, we compare the rest frame peak powers of BL Lacs in terms of the isotropic luminosity peak energy $L_p^* \simeq 4\pi D_L^2 S_p$, where is the luminosity distance (Peebles, 1993). A flat cosmology with $H_0 = 72$ km/(s Mpc), $\Omega_M = 0.27$ and $\Omega_\Lambda = 0.73$ has been used for our calculations (see Spergel et al., 2007, ApJS, 170, 377).
To search for trends, one needs at least 10 observations with E_p, S_p, b well estimated, a requirement satisfied by only 5 of our sources, namely: PKS 0548-322, 1H 1426+418, MRK 501, 1ES 1959+650 and PKS 2155-304. For Mrk 421, the results are $r_{log} = 0.67$ and $r_{log} = -0.67$ for the $E_p^* - L_p^*$ and $E_p^* - b$ relations, respectively.

3.1 1H 1426+428

The source 1H 1426+428 has a similar behaviour to Mrk 421 in the $E_p^* - L_p^*$ and $E_p^* - b$ plots (see Fig. 1a).The observation of *XMM-Newton* on 16 June 2001 appears to confirm the statistical trend in the $E_p^* - b$ plane, even if the bestfit indicates a value of E_p^* beyond the instrumental energy range, but in the $E_p^* - L_p^*$ plane it lies in a different position than other pointings. We find correlation coefficients $r_{log} = 0.72$ for the $E_p^* - L_p^*$ relation, and $r_{log} = -0.47$ for the $E_p^* - b$ one.

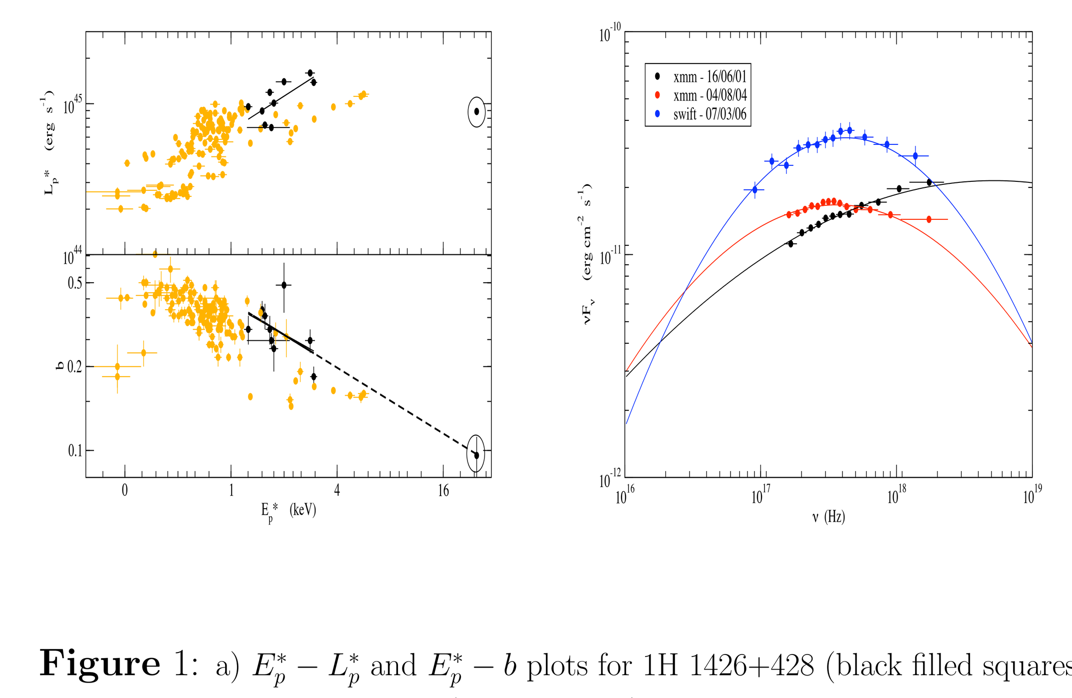

Figure 1: a) $E_p^* - L_p^*$ and $E_p^* - b$ plots for 1H 1426+428 (black filled squares) compared with those of Mrk 421 (orange circles). Black lines indicate the regressions underlying the r_{log} correlation coefficient. Circled values refers to the peculiar observation performed on the 16 June 2001 by *XMM-Newton*. b) The SEDs for three observations of 1H 1426+428 performed by *XMM-Newton* and *Swift*.

3.2 Mrk 501

For Mrk 501 the $E_p^* - L_p^*$ and $E_p^* - b$ plots are shown in Fig. 2. Here the range of E_p^* is wider and the luminosities are higher compared to Mrk 421. The source has similar trends to Mrk 421, with higher correlation coefficients for the $E_p^* - L_p^*$ and $E_p^* - b$ relations, namely, $r_{log} = 0.89$ and $r_{log} = -0.79$, respectively.

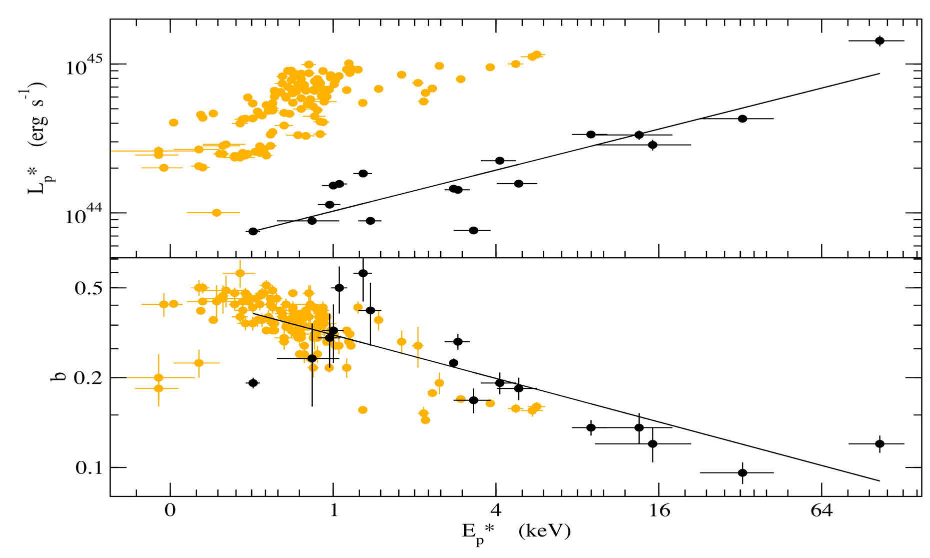

Figure 2: $E_p^* - L_p^*$ and $E_p^* - b$ plots for Mrk 501 (black filled squares) compared with those of Mrk 421 (orange circles). Black lines indicate the regressions underlying the r_{log} correlation coefficient.

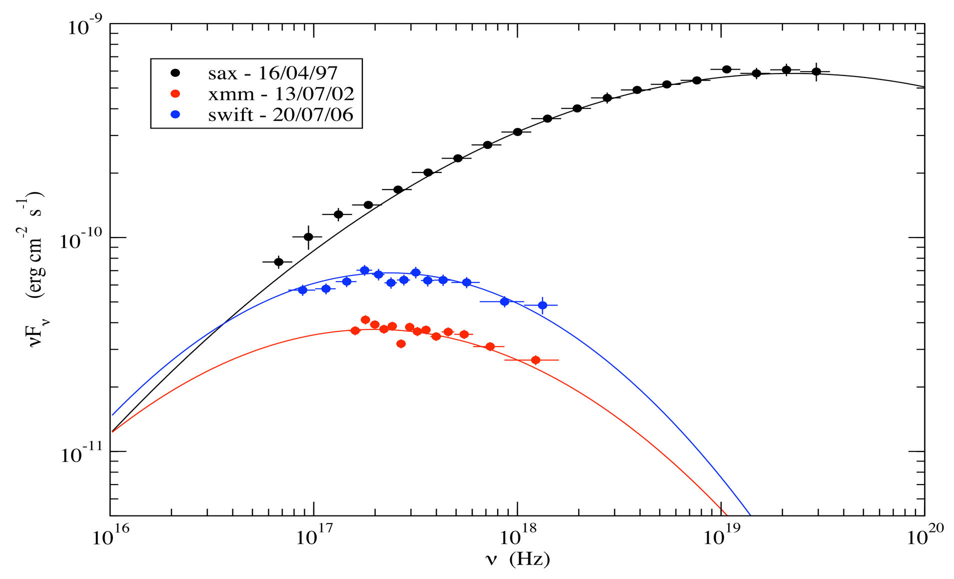

Figure 3: The SEDs for three observations of Mrk 501 performed by *BeppoSAX*, *XMM-Newton* and *Swift*.

3.3 PKS 2155-304

The source PKS 2155-304 is the truly variant member of our set in a number of respects. In fact, the spectral analysis yields a log-parabolic index $a > 2$ (see Eq. 1), and relatedly, $E_p < 1$ keV.

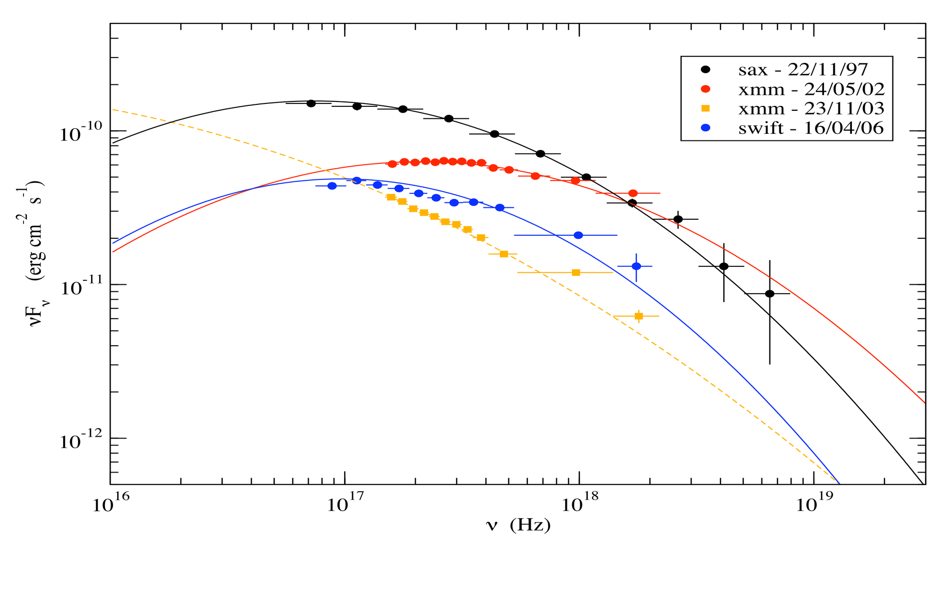

Figure 4: The SEDs for four observations of PKS 2155-304 performed by *BeppoSAX*, *XMM-Newton* and *Swift*.

It was difficult to evaluate the SED peak location with *BeppoSAX*, *XMM-Newton* and *Swift* because it often falls below the observational X-ray range, as shown in Fig. 4. Such spectra indicate that the X rays constitute the upper end of a synchrotron emission. We never observed a high energy exponential cutoff in our analysis, which supports our modelling in terms of a spectral curvature b. The source covers a region in the $E_p^* - b$ plane overlapping that of Mrk 421 in Fig. 5. On the other hand, the same figure shows that the source does not appear to follow a similar trend in the $E_p^* - L_p^*$ plane.

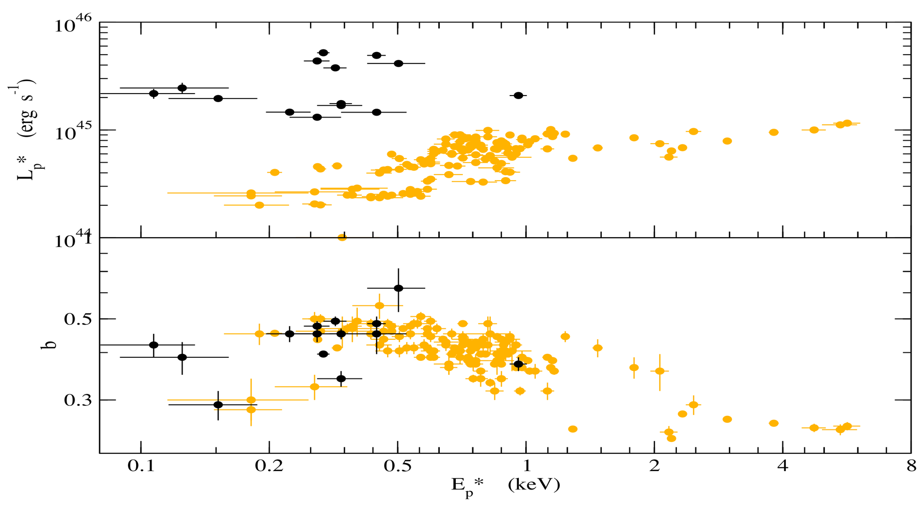

Figure 5: $E_p^* - L_p^*$ and $E_p^* - b$ plots for PKS 2155-304 (black filled squares) compared with those of Mrk 421 (orange circles).

4 Summary

We summarize our main results as follows:

- Five sources (PKS 0548-322, 1H 1426+428, Mrk 501, 1ES 1959+650, PKS2155-304) have enough data to warrant examining in some detail the $E_p^* - L_p^*$ and $E_p^* - b$ relations and comparing them with those found for Mrk 421.
  Comparing these values with those evaluated for Mrk 421 we have found that at least three sources (namely PKS 0548-322, 1H 1426+428 and Mrk 501) follow the same trends as Mrk 421 in the $E_p^* - L_p^*$ plane.
- An overall comparison of these similarities is given in Fig. 6 (upper panel). This portrays the $E_p^* - b$ plane for these five sources plus Mrk 421, to show that the curvature ranges from about 0.12 to about 0.55; the correlation coefficient for the whole sample constituted by these sources is $r_{log} = -0.66$.

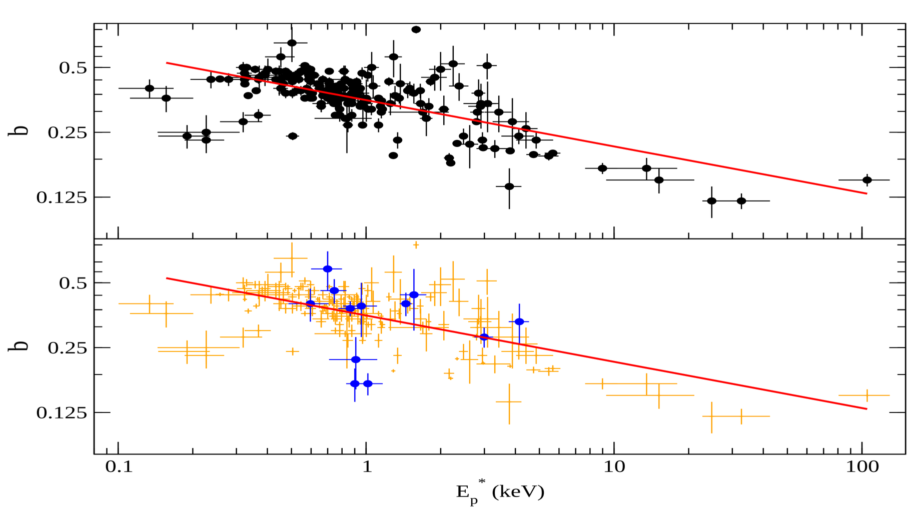

Figure 6: Upper panel: the $E_p^* - b$ plot for Mrk 421 and for the five sources analysed in detail in Sect. 4. Lower panel: blue points represents the other TeV HBLs with insufficient data to perform a detailed analysis. The above sources are replotted with orange crosses.

5 TeV predictions

Correlations between L_p^* and E_p^* provide interesting information concerning the driver of the source spectral evolution. In fact, the synchrotron peak is expected to scale as $L_p^* \propto N\ \gamma^2\ B^2\ \delta^4$ while the peak energy scales as $E_p^* \propto \gamma^2 B\ \delta$, in terms of the number N of emitting particles, the magnetic field B, of the typical electron energy γmc^2, and of the beaming factor δ.
Finally, we outline a link between the synchrotron peak and the TeV emissions. In fact, within a single zone SSC scenario, we expect that synchrotron signatures derived from X-rays observations have counterparts in the TeV energy range, where the inverse Compton peak lies. In closer detail, we expect the inverse Compton peak height C_p^* and its location ϵ_p^* in energy to be given by

$$C_p^* \propto N^2 R^{-2} \gamma^4 B^2 \delta^4 \epsilon_p^* \propto \gamma^4 B \delta \qquad (Thomson\ regime) \qquad (3)$$

$$C_p^* \propto N R^{-2} B \delta^4 \epsilon_p^* \propto \delta\gamma \qquad (Klein-Nishina\ regime), \qquad (4)$$

where R is the size of the emitting region. It transpires that a definite link exists between the correlations for the variations of the synchrotron peak and variability of the inverse Compton peak.